JCTC Journal of Chemical Theory and Computation

Article

pubs.acs.org/JCTC

Numerical Methods for a Kohn−Sham Density Functional Model Based on Optimal Transport

Huajie Chen,* Gero Friesecke, and Christian B. Mendl

Zentrum Mathematik, Technische Universität München, Boltzmannstraβe 3, 85747 Garching bei München, Germany

ABSTRACT: In this paper, we study numerical discretizations to solve density functional models in the "strictly correlated electrons" (SCE) framework. Unlike previous studies, our work is not restricted to radially symmetric densities. In the SCE framework, the exchange-correlation functional encodes the effects of the strong correlation regime by minimizing the pairwise Coulomb repulsion, resulting in an optimal transport problem. We give a mathematical derivation of the self-consistent Kohn−Sham−SCE equations, construct an efficient numerical discretization for this type of problem for $N = 2$ electrons, and apply it to the H_2 molecule in its dissociating limit.

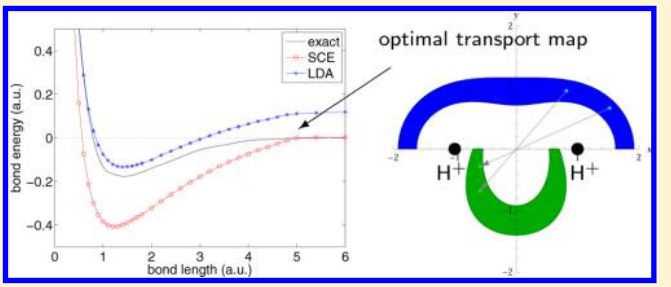

1. INTRODUCTION

In the *ab initio* quantum mechanical modeling of many-particle systems, Kohn−Sham density functional theory (DFT)[1,2] achieves so far the best compromise between accuracy and computational cost and has become the most widely used electronic structure model in molecular simulations and material science. In principle, the ground state energy and electron density of an N-electron system can be obtained by minimizing the Kohn−Sham energy functional. The major drawback of DFT is that the exact functional for the so-called exchange-correlation energy is not known, which includes all the many-particle effects. A basic model is the local density approximation (LDA),[2,3] which is still commonly used in practical calculations. Improvements of this model give rise to the generalized gradient approximation (GGA)[4−6] and hybrid functionals.[7−9] Although these models have achieved high accuracy for many chemical and physical systems, there remain well-known limitations. For example, in systems with significant static correlation,[10] LDA, GGA, and also hybrid functionals underestimate the magnitude of the correlation energy. This becomes particularly problematic for the dissociation of electron pair bonds. An example is the dissociating H_2 molecule: the widely employed LDA, GGA, and even hybrid models fail rather badly at describing the energy curve for dissociating H_2. Many efforts have been made in order to make an appropriate ansatz for the exchange-correlation functional and tackle this problem (e.g., refs 11, 12). In our view, a principal deficiency of these works is the attempt to describe strong correlation within the framework of mean field approximations.

Alternatively, DFT calculations can also be based on the strongly interacting limit of the Hohenberg−Kohn density functional, denoted "strictly correlated electrons" (SCE) DFT.[13,14] This approach considers a reference system with complete correlation between the electrons and is able to capture key features of strong correlation within the Kohn−Sham framework. The pioneering work[14−16] has shown that the SCE ansatz can describe certain model systems in the extreme strongly correlated regime with higher accuracy than standard Kohn−Sham DFT. However, the calculations are presently limited to either one-dimensional or spherically symmetric systems. To our knowledge, there is no SCE-DFT calculation for dissociating the H_2 molecule in $\mathbb{R}^3$. Moreover, the SCE model may be a promising ingredient for future developments of the DFT energy functionals, as it yields qualitative insight into the electron correlations.[17,18] Therefore, it will be necessary to design approximations of SCE physics for general three-dimensional systems.

In the SCE-DFT model, the repulsive energy between strongly interacting electrons is related to optimal transport theory. Optimal transport was historically studied[19] to model the most economical way of moving soil from one area to another and was further generalized[20,21] to the Kantorovich primal and dual formulation. The goal is to transfer masses from an initial density ρ_A to a target density ρ_B in an optimal way such that the "cost" $c(x,y)$ for transporting mass from x to y is minimized (see ref 22 for a comprehensive treatment). The Coulomb repulsive energy in the SCE-DFT model can be reformulated as the optimal cost of an optimal transport problem, if we identify the marginals with the electron density divided by the number of electrons, i.e., ρ/N, and the cost function with the electron−electron Coulomb repulsion

$$c_{ee}(\mathbf{r}_1, ..., \mathbf{r}_N) = \sum_{1\le i<j\le N} \frac{1}{|\mathbf{r}_i - \mathbf{r}_j|} \tag{1}$$

For instance, for a two-electron system within the SCE-DFT framework, the electron repulsive energy for a given single-particle electron density ρ is

Received: July 8, 2014

   dx.doi.org/10.1021/ct500586q | J. Chem. Theory Comput. XXXX, XXX, XXX−XXX

$$V_{ee}^{SCE}[\rho] = \min_{\Psi}\left\{\int_{\mathbb{R}^6} \frac{|\Psi(\mathbf{r}_1, \mathbf{r}_2)|^2}{|\mathbf{r}_1 - \mathbf{r}_2|}\, d\mathbf{r}_1\, d\mathbf{r}_2,\right.$$
$$\left.\int_{\mathbb{R}^3} |\Psi(\mathbf{r}_1, \mathbf{r})|^2\, d\mathbf{r}_1 = \int_{\mathbb{R}^3} |\Psi(\mathbf{r}, \mathbf{r}_2)|^2\, d\mathbf{r}_2 = \frac{\rho(\mathbf{r})}{2}\right\} \quad (2)$$

Strictly speaking, the set of admissible $|\Psi|^2$'s must be enlarged to probability measures in order to allow strict correlation, which corresponds to concentration of the many-body probability density on a lower dimensional subset.[23] There are several mathematical investigations of the relations between SCE-DFT and optimal transport problems, see refs 23−26, but important open problems remain. To our knowledge, the functional derivative of the SCE functional of eq 2 (alias optimal cost functional) with respect to the electron density (alias marginal measure) is not clear from a mathematical point of view. However, this result is crucial for deriving the Kohn−Sham equations needed in practical calculations. Numerical algorithms for optimal transport problems are rather sparse. Explicit solutions for the co-motion functions are known for one-dimensional and spherically symmetric problems[14] but cannot be generalized to nonspherical two- and three-dimensional systems. An alternative route might be the Kantorovich dual formulation of the SCE functional.[24,27] In a complementary work,[28] the H_2 molecule is studied using an ansatz for the dual potential, and there is a recent simulation of a one-dimensional model H_2 molecule using the SCE framework.[18]

In this paper, we give a mathematical derivation of the Kohn−Sham equations for optimal transport-based DFT, which is rigorous up to physically expected uniqueness, smoothness, and continuity assumptions (section 3); provide an efficient numerical algorithm for discretizing and solving the resulting optimal transport problem for the case of two electrons without restriction to radial symmetry (section 4); and then apply this algorithm to a self-consistent DFT simulation of the H_2 molecule in the dissociating limit (section 5). Finally, we show both numerically and by a rigorous mathematical argument that the SCE-DFT model is accurate for the H_2 molecule in the dissociating limit.

2. PRELIMINARIES

Consider a molecular system with M nuclei of charges $\{Z_1,...,Z_M\}$, located at positions $\{\mathbf{R}_1,...,\mathbf{R}_M\}$, and N electrons in the nonrelativistic setting. The electrostatic potential generated by the nuclei is

$$v_{ext}(\mathbf{r}) = -\sum_{I=1}^{M} \frac{Z_I}{|\mathbf{r} - \mathbf{R}_I|},\ \mathbf{r} \in \mathbb{R}^3$$

Within the DFT framework,[1,29] the ground state density and energy of the system is obtained by solving the following minimization problem:

$$E_0 = \min_{\rho}\left\{F_{HK}[\rho] + \int_{\mathbb{R}^3} v_{ext}\rho,\ \rho \geq 0,\ \sqrt{\rho} \in H^1(\mathbb{R}^3),\right.$$
$$\left.\int_{\mathbb{R}^3} \rho = N\right\} \quad (3)$$

where ρ is the electron density and $F_{HK}[\rho]$ is the so-called Hohenberg−Kohn functional.[1] F_{HK} is a universal functional of ρ in the sense that it does not depend on the external potential v_{ext}. Unfortunately, no tractable expression for F_{HK} is known that could be used in numerical simulations. Standard Kohn−Sham DFT[2] treats the system as N noninteracting electrons and approximates $F_{HK}[\rho]$ by the sum of the kinetic energy

$$T_{KS}[\rho] = \inf\left\{\frac{1}{2}\sum_{i=1}^{N}\int_{\mathbb{R}^3} |\nabla\phi_i(\mathbf{r})|^2\, d\mathbf{r},\ \phi_i \in H^1(\mathbb{R}^3),\right.$$
$$\left.\sum_{i=1}^{N} |\phi_i(\mathbf{r})|^2 = \rho(\mathbf{r}),\ \int_{\mathbb{R}^3} \phi_i\phi_j = \delta_{ij}\right\} \quad (4)$$

the Hartree energy $E_H[\rho] = 1/2\int_{\mathbb{R}^3}\int_{\mathbb{R}^3}\rho(\mathbf{r})\rho(\mathbf{r}')|\mathbf{r} - \mathbf{r}'|^{-1}\, d\mathbf{r}\, d\mathbf{r}'$, and an exchange-correlation energy $E_{xc}[\rho]$.

Since the standard noninteracting model cannot capture the features that result from strong correlation, it is not able to simulate strongly correlated electron systems, like the H_2 molecule in its dissociating limit. In contrast to that, the SCE-DFT model[14,30,31] starts from the strongly interacting limit (semiclassical limit) of F_{HK} and gives rise to the following SCE functional (see ref 26 for a mathematical justification)

$$V_{ee}^{SCE}[\rho] = \inf\{V_{ee}[\rho_N],\ \rho_N(\mathbf{r}_1, ..., \mathbf{r}_N) \geq 0,$$
$$\rho_N \text{is symmetric},\ \rho_N \mapsto \rho\} \quad (5)$$

to replace $E_H[\rho] + E_{xc}[\rho]$ in standard Kohn−Sham DFT, where

$$V_{ee}[\rho_N] = \int_{\mathbb{R}^{3N}} c_{ee}(\mathbf{r}_1, \cdots, \mathbf{r}_N)\, \rho_N(\mathbf{r}_1, ..., \mathbf{r}_N)\, d\mathbf{r}_1...d\mathbf{r}_N \quad (6)$$

with c_{ee} given by eq 1, and $\rho_N \mapsto \rho$ means that ρ is the marginal distribution of ρ_N, that is to say

$$\rho(\mathbf{r}) = N\int_{\mathbb{R}^{3(N-1)}} \rho_N(\mathbf{r}, \mathbf{r}_2, ..., \mathbf{r}_N)\, d\mathbf{r}_2...d\mathbf{r}_N$$

The minimization in eq 5 is over all symmetric N-point probability measures ρ_N which have the given single-particle density ρ as marginal and yields the minimum of the electronic Coulomb repulsive energy over all such ρ_N.

The minimization task in eq 5 is in fact an optimal transport problem with Coulomb cost,[23,24,26] which has two alternative formulations: the Monge formulation and the Kantorovich dual formulation. For the Monge formulation, one uses the ansatz

$$\rho_N(\mathbf{r}_1, ..., \mathbf{r}_N) = \frac{\rho(\mathbf{r}_1)}{N}\delta(\mathbf{r}_2 - T_2(\mathbf{r}_1))...\delta(\mathbf{r}_N - T_N(\mathbf{r})) \quad (7)$$

with $T_i:\mathbb{R}^3 \to \mathbb{R}^3$ ($i = 2,...,N$) the so-called co-motion functions (also called optimal transport maps), where we use the convention $T_1(\mathbf{r}) = \mathbf{r}$. The above ansatz already appears on physical grounds, without reference to optimal transport theory, in ref 14. Since the N-particle distribution ρ_N in eq 7 is zero everywhere except on the set

$$M = \{(\mathbf{r}, T_2(\mathbf{r}), ..., T_N(\mathbf{r})),\ \mathbf{r} \in \mathbb{R}^3\} \quad (8)$$

it describes a state where the location of one electron fixes all the other $N - 1$ electrons through the co-motion functions T_i, $i = 2,...,N$. The co-motion functions are implicit functionals of the density, determined by the minimization problem in eq 5 and a set of differential equations that ensure the invariance of the density under the coordinate transformation $\mathbf{r} \mapsto T_i(\mathbf{r})$,[14] i.e.,

$$\rho(T_i(\mathbf{r}))\, dT_i(\mathbf{r}) = \rho(\mathbf{r})\, d\mathbf{r} \quad (9)$$

In terms of these functions, the optimal value of eq 5 reads

dx.doi.org/10.1021/ct500586q | J. Chem. Theory Comput. XXXX, XXX, XXX−XXX

$$V_{ee}^{SCE}[\rho] = \frac{1}{N}\int_{\mathbb{R}^3} \rho(\mathbf{r})\, c_{ee}(T_1(\mathbf{r}), ..., T_N(\mathbf{r}))\, d\mathbf{r} \tag{10}$$

Note that the ansatz eq 7 is not in general symmetric under exchanging particle coordinates; nevertheless, dropping the symmetrization does not alter the minimum value of eq 5.

Alternatively, one can start from the so-called Kantorovich dual formulation.[21,22] It has been shown[24] that the value of $V_{ee}^{SCE}[\rho]$ is exactly given by the maximum of this Kantorovich dual problem

$$V_{ee}^{SCE}[\rho] = \max\left\{\int_{\mathbb{R}^3} u(\mathbf{r})\,\rho(\mathbf{r})\, d\mathbf{r}, \sum_{i=1}^{N} u(\mathbf{r}_i) \le c_{ee}(\mathbf{r}_1, ..., \mathbf{r}_N)\right\} \tag{11}$$

In what follows, we denote the maximizer of eq 11 by u_ρ, which is called the Kantorovich potential. We assume that u_ρ is unique and depends continuously on ρ in the sense that

$$\int_{\mathbb{R}^3} u_{\rho_j}\varphi \to \int_{\mathbb{R}^3} u_\rho\varphi \text{ for all integrable functions } \varphi \text{ if } \int_{\mathbb{R}^3} |\rho_j - \rho| \to 0 \tag{12}$$

In mathematical language, this means u_{ρ_j} converges weakly* to u_ρ in $L^\infty(\mathbb{R}^3)$ if ρ_j tends to ρ in $L^1(\mathbb{R}^3)$.

For numerical implementations, the Kantorovich dual formulation has high complexity due to the $3N$-dimensionality of the constraints. In comparison, the Monge formulation amounts to a spectacular dimension reduction, in which the unknowns are $N-1$ maps on $\mathbb{R}^3$ instead of one function ρ_N on $\mathbb{R}^{3N}$. However, numerical simulations are currently restricted to spherically symmetric densities and one-dimensional systems, for which the intricate constraints 9 can be solved semianalytically. As a first step toward efficient numerical discretization of the Monge formulation, we deal hear with nonspherical systems with $N = 2$ electrons.

3. KOHN–SHAM EQUATIONS FOR OPTIMAL TRANSPORT BASED DFT

By taking V_{ee}^{SCE} as the only interaction term within the Kohn–Sham DFT framework, we can obtain the ground state approximations of energy and electron density by solving the following minimization problem

$$E_0 = \inf_{\Phi}\left\{E_{KS}^{SCE}[\Phi],\ \phi_i \in H^1(\mathbb{R}^3),\ \int_{\mathbb{R}^3}\phi_i\phi_j = \delta_{ij}\right\} \tag{13}$$

where $\Phi = (\phi_1,...,\phi_N)$ denotes the Kohn–Sham orbitals and

$$E_{KS}^{SCE}[\Phi] = \frac{1}{2}\sum_{i=1}^{N}\int_{\mathbb{R}^3}|\nabla\phi_i(\mathbf{r})|^2\, d\mathbf{r} + \int_{\mathbb{R}^3} v_{ext}(\mathbf{r})\,\rho_\Phi(\mathbf{r})\, d\mathbf{r} + V_{ee}^{SCE}[\rho_\Phi] \tag{14}$$

with $\rho_\Phi(\mathbf{r}) = \sum_{i=1}^{N}|\phi_i(\mathbf{r})|^2$. We shall derive the self-consistent Kohn–Sham equations for eq 13 in this section. The key point is to calculate the functional derivative $\delta V_{ee}^{SCE}[\rho]/\delta\rho$ of the SCE functional with respect to the single particle density ρ, which is the effective one-body potential coming from the interaction term. In the derivation below, we make various plausible assumptions on the Kantorovich potential such as uniqueness, continuous dependence on the density, and differentiability at relevant points. We believe these assumptions to be correct except possibly in exceptional situations. A fully rigorous treatment without these assumptions would be desirable but lies beyond the scope of this paper.

Note that the functional $V_{ee}^{SCE}[\rho]$ is not defined on arbitrary densities, but only on those with $\int_{\mathbb{R}^3}\rho = N$. Therefore, the definition of the functional derivative only specifies its integral against perturbations in the corresponding "tangent space", that is to say perturbations that have integral zero:

$$\int_{\mathbb{R}^3}\frac{\delta V_{ee}^{SCE}[\rho]}{\delta\rho}\cdot\tilde{\rho} = \lim_{\varepsilon\to 0}\frac{V_{ee}^{SCE}[\rho+\varepsilon\tilde{\rho}] - V_{ee}^{SCE}[\rho]}{\varepsilon} \quad \text{for all } \tilde{\rho} \text{ with } \int_{\mathbb{R}^3}\tilde{\rho} = 0 \tag{15}$$

The following theorem indicates that the functional derivative is nothing but the Kantorovich potential u_ρ with an additive constant.

Theorem 1. Assume that the Kantorovich potential u_ρ, i.e., the maximizer of eq 11, is unique and depends continuously on the electron density ρ in the sense of eq 12. Then $V_{ee}^{SCE}[\rho]$ is differentiable at ρ, and the functional derivative is given by

$$\frac{\delta V_{ee}^{SCE}[\rho]}{\delta\rho}[\rho] = u_\rho + C \text{ for any constant } C \tag{16}$$

Proof. For any given single-particle density ρ with $\int_{\mathbb{R}^3}\rho = N$, and any perturbation $\tilde{\rho}$ with $\int_{\mathbb{R}^3}\tilde{\rho} = 0$, we define

$$D_\varepsilon = \frac{V_{ee}^{SCE}[\rho+\varepsilon\tilde{\rho}] - V_{ee}^{SCE}[\rho]}{\varepsilon}$$

For simplicity, we assume $\varepsilon > 0$. We have from eq 11 that

$$D_\varepsilon = \frac{\int_{\mathbb{R}^3} u_{\rho+\varepsilon\tilde{\rho}}(\rho+\varepsilon\tilde{\rho}) - \int_{\mathbb{R}^3} u_\rho\rho}{\varepsilon} \tag{17}$$

Using the fact that $u_{\rho+\varepsilon\tilde{\rho}}$ and u_ρ are maximizers of eq 11 with electron density $\rho+\varepsilon\tilde{\rho}$ and ρ, respectively, we have

$$\int_{\mathbb{R}^3} u_\rho(\rho+\varepsilon\tilde{\rho}) \le \int_{\mathbb{R}^3} u_{\rho+\varepsilon\tilde{\rho}}(\rho+\varepsilon\tilde{\rho}) \text{ and } -\int_{\mathbb{R}^3} u_\rho\rho \le -\int_{\mathbb{R}^3} u_{\rho+\varepsilon\tilde{\rho}}\rho \tag{18}$$

Substituting eq 18 into eq 17 gives

$$\int_{\mathbb{R}^3} u_\rho\tilde{\rho} \le \varepsilon D_\varepsilon \le \int_{\mathbb{R}^3} u_{\rho+\varepsilon\tilde{\rho}}\tilde{\rho} \tag{19}$$

Under the uniqueness and continuity assumption eq 12, the right-hand side of eq 19 converges to the left-hand side as $\varepsilon \to 0$. Hence, for any $\tilde{\rho}$ with $\int_{\mathbb{R}^3}\tilde{\rho} = 0$, $\lim_{\varepsilon\to 0} D_\varepsilon$ exists and equals $\int_{\mathbb{R}^3} u_\rho\tilde{\rho}$. This together with definition 15 leads to $v_{SCE}[\rho] = u_\rho$.

Note that the map $\tilde{\rho} \mapsto \int_{\mathbb{R}^3}((\delta V_{ee}^{SCE}[\rho])/\delta\rho)\tilde{\rho}$ is unique up to an additive constant since $\int_{\mathbb{R}^3}\tilde{\rho} = 0$. Therefore, the functional derivative viewed as a function can be modified by any additive constant C. This completes the proof.

The following theorem shows that the Kantorovich potential u_ρ is related to the co-motion functions in the Monge formulation. With respect to an at first sight different notion of effective one-body potential, this was noted and justified in ref 14. Our proof in Appendix A proceeds by combining the

dx.doi.org/10.1021/ct500586q | J. Chem. Theory Comput. XXXX, XXX, XXX–XXX

result of ref 14 with a proof that their notion of effective potential actually coincides with the Kantorovich potential.

Theorem 2. Let ρ_N be the minimizer of the optimal transport problem eq 5 with given single-particle density ρ and any interaction $c_{ee}(\mathbf{r}_1,\mathbf{r}_2,...,\mathbf{r}_N)$. If u_ρ is the Kantorovich potential, i.e., the maximizer of eq 11, and u_ρ is differentiable, then

$$\nabla u_\rho(\mathbf{r}) = \nabla_{\mathbf{r}} c_{ee}(\mathbf{r}, \mathbf{r}_2, ..., \mathbf{r}_N) \text{ on } \mathrm{supp}(\rho_N) \tag{20}$$

In particular, if ρ_N is of the Monge form eq 7, then $\mathrm{supp}(\rho_N) = M$ (see eq 8) and

$$\nabla u_\rho(\mathbf{r}) = \nabla_{\mathbf{r}} c_{ee}(\mathbf{r}, \mathbf{r}_2, ..., \mathbf{r}_N)|_{\mathbf{r}_2=T_2(\mathbf{r}),...,\mathbf{r}_N=T_N(\mathbf{r}_N)} \tag{21}$$

i.e., in the standard case of Coulomb repulsion in eq 1,

$$\nabla u_\rho(\mathbf{r}) = -\sum_{i=2}^{N} \frac{\mathbf{r} - T_i(\mathbf{r})}{|\mathbf{r} - T_i(\mathbf{r})|^3} \tag{22}$$

In case $N = 2$, there is only one co-motion function T, and

$$\nabla u_\rho(\mathbf{r}) = -\frac{\mathbf{r} - T(\mathbf{r})}{|\mathbf{r} - T(\mathbf{r})|^3} \tag{23}$$

Note that solving this equation for $T(\mathbf{r})$ gives an instance of the celebrated Gangbo–McCann formula[32] for the optimal map in terms of the Kantorovich potential. For the Coulomb cost, this formula takes the form[23]

$$T(\mathbf{r}) = \mathbf{r} + \frac{\nabla u_\rho(\mathbf{r})}{|\nabla u_\rho(\mathbf{r})|^{3/2}} \tag{24}$$

However, unlike eq 24, formula 23 generalizes (in the form of eq 22) to many-body or multimarginal problems. Thus, formula 22 (or 21) should be viewed as the correct generalization of the Gangbo–McCann formula to multimarginal problems; note also that our derivation works for general costs $c_{ee}(\mathbf{r}_1,...,\mathbf{r}_N)$.

Theorems 1 and 2 yield the Kohn–Sham equations corresponding to the SCE energy functional 14 with a computable effective potential. They are the Euler–Lagrange equations corresponding to the minimization problem 13 (after a unitary transformation to diagonalize the symmetric $N \times N$ matrix of Lagrange multipliers): find $\lambda_i \in \mathbb{R}, \phi_i \in H^1(\mathbb{R}^3)(i = 1,2,...,N)$ such that

$$\begin{cases} \left(-\frac{1}{2}\Delta + v_{\mathrm{ext}} + u_{\rho_\Phi}\right)\phi_i = \lambda_i\phi_i \text{ in } \mathbb{R}^3, \\ \qquad\qquad i = 1, 2, ..., N \\ \int_{\mathbb{R}^3} \phi_i\phi_j = \delta_{ij} \end{cases} \tag{25}$$

This is a nonlinear eigenvalue problem, where the potential u_{ρ_Φ} depends on the electron density ρ_Φ associated with the orbitals ϕ_i. A self-consistent field (SCF) iteration algorithm is commonly resorted to for this nonlinear problem. In each iteration step of the algorithm, a new effective potential is constructed from a trial electron density and a linear eigenvalue problem is then solved to obtain the low-lying eigenvalues.

We shall comment further on the additive constant in eq 16. Modifying u_{ρ_Φ} by an arbitrary additive constant yields the same Kohn–Sham orbitals ϕ_i and only leads to a corresponding shift of the nonlinear eigenvalues λ_i. However, as pointed out in ref 26, it is only when the effective potential is precisely the Kantorovich potential that the ground state energy equals the sum of Kohn–Sham eigenvalues, i.e., $E_0 = \Sigma_{i=1}^N \lambda i$.

4. NUMERICAL DISCRETIZATIONS OF OPTIMAL TRANSPORTATION

In each iteration of the SCF algorithm for solving eq 25, one has to construct $u_{\tilde\rho}$ from a trial electron density $\tilde\rho$. According to eq 22, this requires the solution of the optimal transport problem 5 with a given single-particle density to obtain the co-motion functions T_i, $i = 2,...,N$. For simplicity, we only consider the case $N = 2$, where only one co-motion function has to be calculated (which is denoted by T in the following). For systems with more than two electrons, we refer to section 6 for a future perspective.

We discretize the computational domain into n finite elements $e_1,...,e_n$. (We replace $\mathbb{R}^3$ by a bounded domain so that it can be discretized into a finite number of elements. This is reasonable since the electron density $\rho(\mathbf{r})$ of a confined system decays exponentially fast to zero as $|\mathbf{r}| \to \infty$.)[33] Each element is represented by a point $\mathbf{a}_k$ located at its barycenter and its electron mass $\rho_k = \int_{e_k} \rho(\mathbf{r})\, d\mathbf{r}$. Within this discretization, we can approximate the two-particle density $|\Psi(\mathbf{r}_1,\mathbf{r}_2)|^2$ by a matrix $X = (x_{kl}) \in \mathbb{R}^{n\times n}$ with $x_{kl} = |\Psi(\mathbf{a}_k,\mathbf{a}_l)|^2$. (Alternatively, one could identify the entries with the average $x_{kl} = 1/(|e_k|\cdot|e_l|) \int_{e_k}\int_{e_l} |\Psi(\mathbf{r}_1,\mathbf{r}_2)|^2\, d\mathbf{r}_1\, d\mathbf{r}_2$.) The continuous problem 5 is then discretized into

$$\begin{aligned} \min_X \quad & \sum_{1\le k,l\le n} \frac{x_{kl}}{|\mathbf{a}_k - \mathbf{a}_l|} \\ s.\,t. \quad & \sum_{1\le k\le n} x_{kl} = \frac{1}{2}\rho_k,\ l = 1, ..., n \\ & \sum_{1\le l\le n} x_{kl} = \frac{1}{2}\rho_l,\ k = 1, ..., n \\ & x_{kl} \ge 0 \end{aligned} \tag{26}$$

Note that eq 26 is a linear programming problem of the form

$$\min_x f^T x$$

$$\text{s. t. } Ax = b \text{ and } x_k \ge 0$$

where x is the vector containing the entries of X. We can solve this problem by standard optimization routines like *"linprog"* in Matlab. Due to the symmetry of the problem, one can assume that $x_{lk} = x_{kl}$ and only needs to consider x_{kl} for $k \le l$.

As a remark, the dual problem of eq 26 (in the sense of linear programming) results in a discretized version of the Kantorovich dual formulation 11.

The solution of eq 26 entails an approximation of the co-motion functions at the barycenters $\{\mathbf{a}_k\}_{1\le k\le n}$ via the matrix $\mathbf{X} = (x_{kl})$:

$$T_n(\mathbf{a}_k) = \sum_{l=1}^{n} \mathbf{a}_l \frac{2x_{kl}}{\rho_l},\ k = 1, ..., n \tag{27}$$

where x_{kl} can also be regarded as the mass of electron transported from $\mathbf{a}_k$ to $\mathbf{a}_l$. If the discretization is sufficiently fine, i.e., n is large enough, then T_n is a good approximation of T.

For a *uniform* discretization $\{e_k\}_{1\le k\le n}$, the number of degrees of freedom for linear programming eq 26 may be huge. To reduce the computational cost, we use a locally refined mesh instead, which has more elements where the electron density is high and less elements where the electron density is low. Generally speaking, the optimal mesh may be such that each

dx.doi.org/10.1021/ct500586q | J. Chem. Theory Comput. XXXX, XXX, XXX–XXX

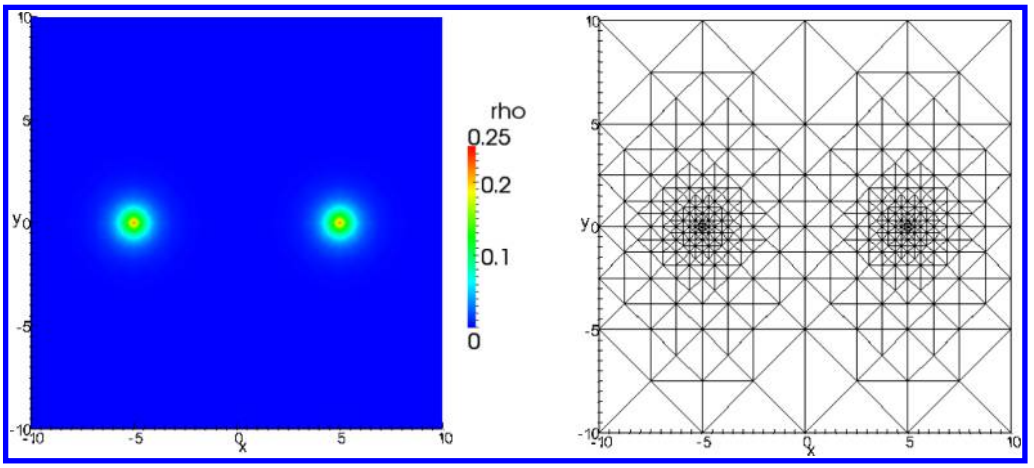

Figure 1. Electron density and corresponding mesh on slice $z = 0$ ($R = 5$).

element e_k has almost equal electron mass ρ_k. This type of mesh can be generated by an adaptive procedure; say, one refines the element when its electron mass is larger than a given threshold and coarses it otherwise. Since the electron density decays exponentially fast to zero as $|\mathbf{r}| \to \infty$, the mesh is much coarser far away from the nuclei than close to the nuclei, which reduces the degrees of freedom significantly.

As a remark, let us assume for a moment that all elements have exactly the same mass, $\rho_k = \overline{\rho}$ for all k. Then the constraints in eq 26 force X to be a *doubly stochastic* matrix (up to a global scaling factor) with non-negative entries. According to Birkhoff's theorem, the extremal points of the convex set of admissible matrices X are the permutations, i.e., matrices with exactly one nonzero entry $\overline{\rho}/2$ in each row (or column). Since the optimum is obtained at an extremal point, the optimizer can be chosen of this form. We have thus derived a discrete analogue of the Monge formulation, since the sum on the right of eq 27 will have exactly one nonzero term.

Another important technique to reduce the computational cost is to exploit the symmetry of the system. If the electron density ρ has some kind of symmetric property, then we can reduce the computations to some subdomain accordingly. For example, ref 14 gives an explicit formula of co-motion functions for spherically symmetric electron densities by making use of the symmetry. More precisely, it is proven that if the density has the form $\rho(\mathbf{r}) = h(|\mathbf{r}|)$ with some function $h:[0,\infty) \to \mathbb{R}$, then the corresponding co-motion function T has to be spherically symmetric itself, that is

$$T(\mathbf{r}) = g(|\mathbf{r}|)\frac{\mathbf{r}}{|\mathbf{r}|}, \ \forall\ \mathbf{r} \in \mathbb{R}^3$$

with some function $g:[0,\infty) \to \mathbb{R}$. This reduces the three-dimensional spherically symmetric problem into a one-dimensional problem.

Here, we consider cylindrically symmetric systems, for instance, diatomic molecules. The following theorem states that the co-motion function T inherits the cylindrical symmetry of the density, which can be proved by using similar arguments to those in the discussion of spherical symmetry in ref 26.

Theorem 3. Let $N = 2$ and denote the cylindrical coordinates by (γ,φ,z). If $\rho(\mathbf{r}) = \varrho(\gamma,z)$ with some function ϱ: $[0,\infty) \times \mathbb{R} \to \mathbb{R}$, then the corresponding co-motion function T satisfies

$$T\colon (\gamma, \varphi, z) \mapsto (\gamma', \varphi + \pi, z')\ \forall\ (\gamma, z) \in [0, \infty) \times \mathbb{R} \tag{28}$$

where $(\gamma',z') = l(\gamma,z)$ with some map $l:[0,\infty) \times \mathbb{R} \to [0,\infty) \times \mathbb{R}$.

An important application of the numerical methods introduced above is to simulate the H_2 molecule at its dissociating limit. We provide more details in the next section.

5. H_2 BOND DISASSOCIATION

We now consider the H_2 molecule. Let $R > 0$ and $\mathbf{R}_A = (-R,0,0)$, $\mathbf{R}_B = (R,0,0)$ be the locations of two hydrogen atoms. Physically, the hydrogen molecule should dissociate into two free hydrogen atoms as the bond length $2R \to \infty$, with the ground state spin-unpolarized. The spin-restricted Hartree–Fock and Kohn–Sham DFT models give the correct spin multiplicity but overestimate total energies, i.e., higher than that of two free hydrogen atoms. In comparison, the spin-unrestricted models give fairly good total energies, while the wave functions are spin-contaminated, which is known as "symmetry breaking" in H_2 bond dissociation.

Here we focus on the SCE-DFT model without symmetry breaking and show both theoretically and numerically that the restricted Kohn–Sham model eq 13 gives the correct ground state energy in the dissociation limit $R \to \infty$. Denote by e_0 the ground state energy of a single hydrogen atom

$$e_0 = \inf\left\{\frac{1}{2}\int_{\mathbb{R}^3} |\nabla\phi(\mathbf{r})|^2\, \mathrm{d}\mathbf{r} - \int_{\mathbb{R}^3} \frac{|\phi(\mathbf{r})|^2}{|\mathbf{r}|}\, \mathrm{d}\mathbf{r},\ \phi \in H^1(\mathbb{R}^3),\ \|\phi\|_{L^2(\mathbb{R}^3)} = 1\right\} \tag{29}$$

$E_{\mathrm{SCE}}(R)$ denotes the ground state energy of the hydrogen molecule in the SCE-DFT model eq 14

$$E_{\mathrm{SCE}}(R) = \frac{1}{2R} + \inf\left\{\int_{\mathbb{R}^3} |\nabla\phi(\mathbf{r})|^2\, \mathrm{d}\mathbf{r} + 2\int_{\mathbb{R}^3} v_{\mathrm{ext}}(\mathbf{r})|\phi(\mathbf{r})|^2\, \mathrm{d}\mathbf{r} + V_{\mathrm{ee}}^{\mathrm{SCE}}[2|\phi|^2],\ \phi \in H^1(\mathbb{R}^3),\ \|\phi\|_{L^2(\mathbb{R}^3)} = 1\right\} \tag{30}$$

where $v_{\mathrm{ext}}(\mathbf{r}) = -|\mathbf{r} - \mathbf{R}_A|^{-1} - |\mathbf{r} - \mathbf{R}_B|^{-1}$. The following result indicates that the SCE-DFT model is correct for the H_2 molecule at its dissociating limit. The rigorous proof is given in Appendix B.

Theorem 4. Let e_0 and $E_{\mathrm{SCE}}(R)$ be given by eqs 29 and 30, respectively. We have

$$\lim_{R\to\infty} E_{\mathrm{SCE}}(R) = 2e_0 \tag{31}$$

dx.doi.org/10.1021/ct500586q | J. Chem. Theory Comput. XXXX, XXX, XXX–XXX

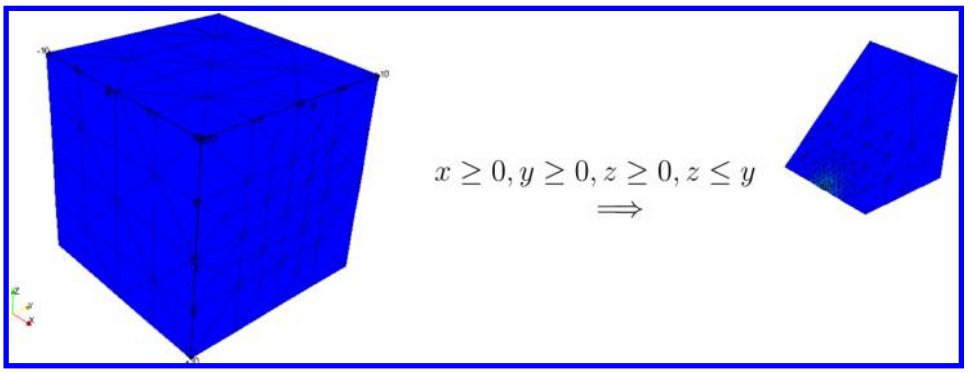

Figure 2. Symmetric decomposition of the computation domain Ω for H_2.

In what follows, we present a numerical simulation of the dissociating H_2 molecule to support the theory. The computations are carried out on a bounded domain $\Omega = [-10,10]^3$. We use an SCF algorithm to solve eq 25 for the ground state energies and electron densities for different bond lengths $2R$. Concerning the optimal transport problem, we use the numerical methods introduced in section 4 and calculate the co-motion function in each SCF iteration step. The nonuniform mesh is generated by the package PHG,[34] a toolbox for parallel adaptive finite element programs developed at the State Key Laboratory of Scientific and Engineering Computing of the Chinese Academy of Sciences. While the problem is effectively two-dimensional according to Theorem 3, we have performed the calculations in three dimensions since PHG is tailored to three-dimensional problems. Figure 1 shows a contour plot of the electron density at slice $z = 0$ and the corresponding mesh. One observes that the grid reflects the higher density around the nuclei.

To further reduce the computational cost, we can exploit the cylindrical symmetry of the system with the help of Theorem 3. As shown in Figure 2, the degrees of freedom can be reduced to 1/16 of the original volume. For the linear programming problem eq 26, we resort to MOSEK,[35] high-performance software for large-scale optimization problems.

The computational results are presented in Figure 3, in which we compare the bond energies in dependence on R using the LDA and SCE Kohn–Sham methods (with exact data from ref 36). Here, the bond energies are the ground state energies of the systems minus $2e_0$, which is expected to be zero when the two hydrogen atoms are disassociated. Note that the SCE model shows the correct asymptotic behavior, while the LDA model fails at large R by giving too large energies. For comparison, the LDA error 0.065 au in ref 37 for the infinitely stretched H_2 molecule is lower than that in Figure 3 since twice the LDA-hydrogen energy is subtracted instead of twice the exact e_0, but it remains significant; errors of similar magnitude are reported there for other functionals such as B3LYP or PBE.

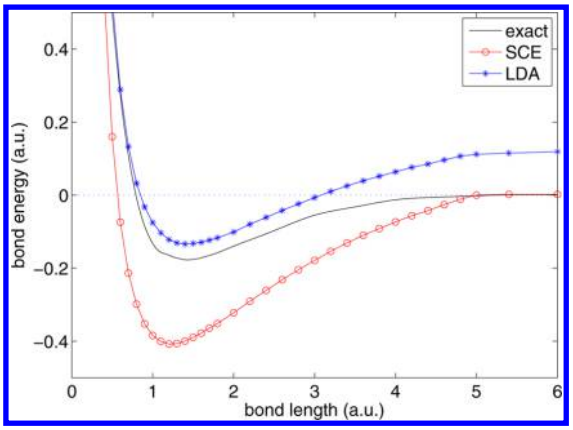

Figure 3. Dissociation energy curves of H_2 for the exact (see ref 36), SCE, and LDA models.

A physical explanation for these results is as follows. At long internuclear separations, if one electron is located near atom A, the other will be found close to atom B. This correlation is correctly reflected by the optimal transport model; hence the SCE model gives asymptotically the same energy as the product of hydrogen orbitals on the two nuclei. In contrast, within the Kohn–Sham LDA framework, the two electrons are constrained to be in the same spatial orbital and do not experience the position of each other. The possibility of both electrons being on the same position is not excluded, resulting in the wrong asymptotic behavior of the disassociation energy in Figure 3.

We also observe from Figure 3 that the SCE model underestimates the ground state energy badly near the equilibrium. The reason is that the SCE approach takes the minimum of the kinetic and Coulomb repulsive energy separately, yielding a lower bound of the exact Hohenberg–Kohn functional. This approach therefore gives rise to considerable error since the minimizers of the two parts usually have very different structures. The SCE-DFT calculations overlocalize electrons and miss the shell structure. Despite the failure of the SCE model near the equilibrium, we believe that it is a promising ingredient in future DFT functionals, which aim to provide accurate approximations in all correlation regimes (see some recent works in refs 17, 18).

We further compare the electron densities and effective potentials obtained by the two different models in Figure 4. The electron densities are actually quite close, while the shape of the potentials differs substantially when R is large. The SCE potential is larger between the hydrogen atoms, favoring a depletion of the bond charge as the two atoms separate. This produces the correct results for large R.

Finally, as an illustration of the co-motion function or optimal map, Figure 5 shows the image under the map of a density contour.

6. CONCLUSIONS AND PERSPECTIVES

The numerical discretization of the general SCE optimal transport problem with Coulomb cost and two marginals leads to the linear programming problem eq 26, which can indeed be solved in practice, as we have demonstrated in a proof of

dx.doi.org/10.1021/ct500586q | J. Chem. Theory Comput. XXXX, XXX, XXX−XXX

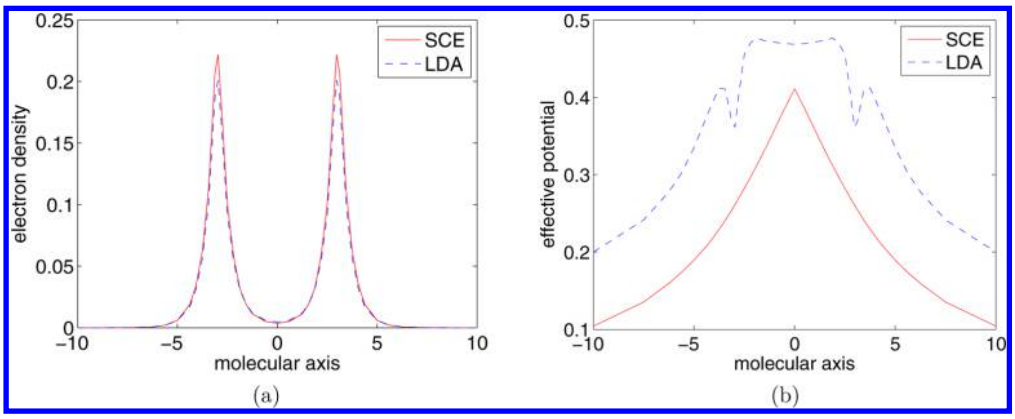

Figure 4. SCE and LDA electron densities (a) and potentials (b) of H_2, plotted along the molecular axis.

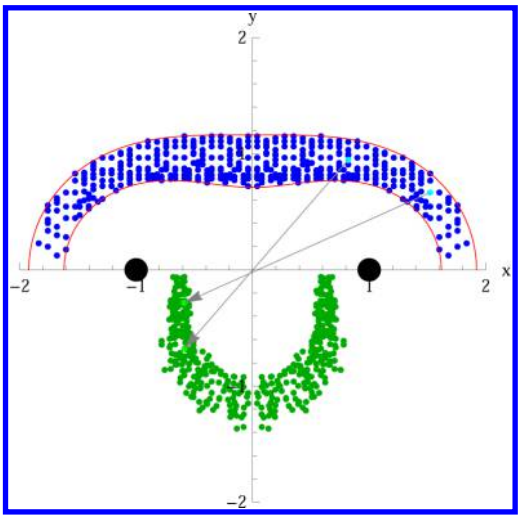

Figure 5. Optimal transport mapping of the region $0.04 \le \rho(\mathbf{r}) \le 0.08$ (indicated by the blue dots inside the red contours) to the green area, for the H_2 molecule with $R = 1$. Each blue dot corresponds to one barycenter in the numerical discretization and has been rotated into the $x-y$ plane with $y \ge 0$ for visual clarity. The green dots are precisely the images of the blue dots under the optimal transport map.

concept calculation. The self-consistent SCE-DFT simulation of the H_2 binding curve agrees well with the exact curve at the dissociating limit but is inferior to standard DFT models like LDA near equilibrium. However, progress in DFT has often relied on combining or hybridizing asymptotic functionals coming from different asymptotic regimes, we therefore believe that for future development of the DFT energy functionals, the SCE model is a promising ingredient.

The theory of this paper applies to more general systems with arbitrary numbers of electrons; however, the numerical algorithms need further development. Specifically, we can restrict the N-particle density to the ansatz

$$\rho_N(\mathbf{r}_1, \ldots, \mathbf{r}_N) = \frac{\rho(\mathbf{r}_1)}{N}\gamma_2(\mathbf{r}_1, \mathbf{r}_2)\gamma_3(\mathbf{r}_1, \mathbf{r}_3)\ldots\gamma_N(\mathbf{r}_1, \gamma_N)$$

where ρ is the given single-particle density. Here, $\gamma_j(\mathbf{r}_1,\mathbf{r}_j)$ represents the probability of the jth electron being found at $\mathbf{r}_j$ while the first electron is located at $\mathbf{r}_1$. We have

$$\int_{\mathbb{R}^3} \gamma_j(\mathbf{r}_1, \mathbf{r}_j)\, d\mathbf{r}_j = 1 \quad j = 2, \ldots, N$$

With a given discretization $\{e_k\}_{1\le k\le n}$ and barycenters $\mathbf{a}_k$ of e_k, we can approximate $\gamma_j(\mathbf{r}_1,\mathbf{r}_j)$ by a matrix $X_j = (x_{j,kl}) \in \mathbb{R}^{n\times n}$ for $j = 2,\ldots,N$. Then the continuous model eq 5 is reduced to

$$\begin{aligned}
\min_{X_2,\ldots,X_N} \quad & \sum_{1<j\le N}\sum_{k,l=1}^{n} \frac{x_{j,kl}}{|\mathbf{a}_k - \mathbf{a}_l|}\cdot\frac{\rho_k}{N} \\
& + \sum_{1<i<j\le N}\sum_{k,l,l'=1}^{n} \frac{x_{i,kl}\cdot x_{j,kl'}}{|\mathbf{a}_l - \mathbf{a}_{l'}|}\cdot\frac{\rho_k}{N} \\
\text{s. t.} \quad & \sum_{k=1}^{n} x_{i,kl} = 1,\ l = 1, \ldots, n,\ i = 2, \ldots, N \\
& \sum_{l=1}^{n} x_{i,kl} = 1,\ k = 1, \ldots, n,\ i = 2, \ldots, N \\
& x_{i,kl} \ge 0
\end{aligned} \tag{32}$$

This is a quadratic programming problem of the form

$$\min_x x^T H x + f^T x$$

$$\text{s. t. } Ax = b \text{ and } x_k \ge 0$$

By solving the above quadratic programming problem, we approximate the co-motion functions $T_2,\ldots,T_N$ by the matrices $X_2 = (x_{2,kl}),\ldots,X_N = (x_{N,kl})$. Similar to eq 27, the co-motion functions can be approximated by

$$T_i(\mathbf{a}_k) \approx \sum_{1\le l\le n} \mathbf{a}_l x_{i,kl} \quad k = 1, \ldots, n,\ i = 2, \ldots, N$$

However, a serious difficulty in solving eq 32 stems from the nonconvexity of the matrix H. Moreover, the symmetry properties as in Theorem 3 are not clear for systems with symmetric densities but more than two electrons. We plan to investigate these issues in future work.

APPENDIX

A. Proof of Theorem 2

First, since $V_{ee}^{SCE}[\rho]$ is easily seen to be convex, it equals its double Legendre transform. Second, the constraint $\rho_N \mapsto \rho$ can been eliminated from the first Legendre transform:

dx.doi.org/10.1021/ct500586q | J. Chem. Theory Comput. XXXX, XXX, XXX−XXX

$$-V_{ee}^{SCE*}[v] = \min_{\rho}(V_{ee}^{SCE}[\rho] - \int_{\mathbb{R}^3} v\rho) = \min_{\rho}\min_{\rho_N \mapsto \rho}\left(\int_{\mathbb{R}^{3N}} c_{ee}\rho_N - \int_{\mathbb{R}^3} v\rho\right) = \min_{\rho_N \mapsto \rho}\int_{\mathbb{R}^{3N}} \rho_N(\mathbf{r}_1, ..., \mathbf{r}_N)\left(c_{ee}(\mathbf{r}_1, ..., \mathbf{r}_N) - \sum_{i=1}^{N} v(\mathbf{r}_i)\right) \quad (33)$$

This results in the following variational principle introduced in ref 14:

$$V_{ee}^{SCE}[\rho] = \max_{v}\left(\int_{\mathbb{R}^3} v\rho + \min_{\rho_N}\int_{\mathbb{R}^{3N}}\left(c_{ee} - \sum_{i=1}^{N} v(\mathbf{r}_i)\right)\rho_N\right) \quad (34)$$

As noted in ref 14, the support of any minimizer $\tilde{\rho}_N$ of the inner minimization must be contained in the set of absolute minimizers of $c_{ee}(\mathbf{r}_1,...,\mathbf{r}_N) - \sum_{i=1}^{N} v(\mathbf{r}_i)$, yielding

$$\nabla_{\mathbf{r}_i} c_{ee}(\mathbf{r}_1, ..., \mathbf{r}_N) - \nabla_{\mathbf{r}_i} v(\mathbf{r}_i) = 0 \text{ on } \mathrm{supp}(\tilde{\rho}_N) \quad (35)$$

Next, we claim that if v_0 is a maximizer of eq 34, then the corresponding minimizer ρ_N^0 of the inner optimization of eq 34 is exactly the minimizer of the original problem eq 5. To see this, use the necessary condition for maximization of v_0 that

$$0 = \frac{d}{d\varepsilon}\bigg|_{\varepsilon=0}\left(\int_{\mathbb{R}^3}(v_0 + \varepsilon\tilde{v})\rho + \min_{\rho_N}\int_{\mathbb{R}^{3N}}\left(c_{ee} - \sum_{i=1}^{N} v_0(\mathbf{r}_i) - \varepsilon\sum_{i=1}^{N}\tilde{v}(\mathbf{r}_i)\right)\rho_N\right) \quad (36)$$

for any $\tilde{v}$, infer from first order perturbation theory that to first order the minimum is given by $\int_{\mathbb{R}^{3N}}(c_{ee} - \sum_{i=1}^{N} v_0(\mathbf{r}_i))\rho_N^0 + \int_{\mathbb{R}^{3N}} \sum_{i=1}^{N}\tilde{v}(\mathbf{r}_i)\rho_N^0$ with ρ_N^0 being the minimizer for $\varepsilon = 0$ and conclude that ρ_N^0 automatically has marginal ρ. This yields eq 35 with v replaced by v_0 and $\tilde{\rho}_N$ replaced by ρ_N^0.

In order to obtain eq 20, it is now only necessary to show that $u_\rho(\mathbf{r}) = v_0(\mathbf{r}) + \mu$ for some constant μ. Using that the maximum value of eq 34 is invariant under changing v by an additive constant, the maximization over v in eq 34 may be restricted to v's with the additional property

$$\min_{(\mathbf{r}_1,...,\mathbf{r}_N)\in\mathbb{R}^{3N}}\left(c_{ee}(\mathbf{r}_1, ..., \mathbf{r}_N) - \sum_{i=1}^{N} v(\mathbf{r}_i)\right) = 0 \quad (37)$$

For these v's, the minimization over ρ_N in eq 34 can be carried out explicitly, yielding

$$V_{ee}^{SCE}[\rho] = \max\left\{\int_{\mathbb{R}^3} v\rho,\ v \text{ satisfies } 37\right\} \quad (38)$$

This maximum value remains unchanged when replacing eq 37 by the inequality constraint in eq 11, which completes the proof.

B. Proof of Theorem 4

First, we establish an upper bound on $E_{SCE}(R)$. Let $\varphi(r) = e^{-r}/\sqrt{\pi}$ and

$$\psi(\mathbf{r}) = \left(\frac{1}{2}(\varphi^2(|\mathbf{r} - \mathbf{R}_A|) + \varphi^2(|\mathbf{r} - \mathbf{R}_B|))\right)^{1/2}$$

Note that φ is the minimizer of eq 29, and $\|\varphi\|_{L^2(\mathbb{R}^3)} = 1$ implies $\|\psi\|_{L^2(\mathbb{R}^3)} = 1$, we have

$$E_{SCE}(R) \le \frac{1}{2R} + \int_{\mathbb{R}^3}|\nabla\psi(\mathbf{r})|^2\,d\mathbf{r} + 2\int_{\mathbb{R}^3} v_{ext}(\mathbf{r})|\psi(\mathbf{r})|^2\,d\mathbf{r} + V_{ee}^{SCE}[2|\psi|^2] \quad (39)$$

which together with the fact that

$$V_{ee}^{SCE}[2|\psi|^2] \le \int_{\mathbb{R}^6}\frac{2|\psi(\mathbf{r}_1)|^2\delta(\mathbf{r}_2, -\mathbf{r}_1)}{|\mathbf{r}_1 - \mathbf{r}_2|}\,d\mathbf{r}_1\,d\mathbf{r}_2 = O(R^{-1}) \quad (40)$$

a direct calculation leads to $E_{SCE}(R) \le 2e_0 + O(R^{-1})$.

For the lower bound of $E_{SCE}(R)$, we observe that $E_{SCE}(R) \ge 1/2R + 2\inf_{\|\phi\|_{L2}=1}\langle\phi|\hat{h}|\phi\rangle$, where $\hat{h}$ is the H_2^+ Hamiltonian $\hat{h} = -1/2\Delta + v_{ext}$. We claim that

$$\langle\phi|\hat{h}|\phi\rangle \ge (e_0 - O(R^{-1}))\|\phi\|_{L^2}^2 \ \forall\ \phi \in H^1(\mathbb{R}^3) \quad (41)$$

To see this, we first decompose the unity function on $\mathbb{R}$ into two smooth cutoff functions $\tilde{\zeta}_1$ and $\tilde{\zeta}_2$, such that $\tilde{\zeta}_1^2 + \tilde{\zeta}_2^2 = 1$, $\tilde{\zeta}_1(x) = 0$ for $x < -1/2$, $\tilde{\zeta}_2(x) = 0$ for $x > 1/2$, and $|\nabla\tilde{\zeta}_i| \le C^*$ with some constant C^*. Let

$$\zeta_i(\mathbf{r}) = \zeta_i(x, y, z) = \tilde{\zeta}_i(x/R) \quad i = 1, 2$$

and $\phi_i = \zeta_i\phi$. Using this relationship, its consequence that $\Sigma_{i=1}^2|\nabla\phi_i|^2 = \Sigma_{i=1}^2(|\nabla\zeta_i|^2)|\phi|^2 + |\nabla\phi|^2$, and the fact $|\nabla\zeta_i| \le C^*/R$, we have

$$\langle\phi|\hat{h}|\phi\rangle \ge \sum_{i=1}^{2}\int_{\mathbb{R}^3}\left(\frac{1}{2}|\nabla\phi_i|^2 - \frac{|\phi_i|^2}{|\mathbf{r}|}\right) - \left(\frac{C^*}{R}\right)^2 - \frac{2}{R}$$

which implies eq 41. Considering the upper and lower bounds completes the proof of eq 31.

AUTHOR INFORMATION

Corresponding Author

*E-mail: chenh@ma.tum.de.

Notes

The authors declare no competing financial interest.

ACKNOWLEDGMENTS

C.M. acknowledges support from the DFG project FR 1275/3-1.

REFERENCES

(1) Hohenberg, P.; Kohn, W. *Phys. Rev. B* **1964**, *136*, 864−871.
(2) Kohn, W.; Sham, L. J. *Phys. Rev.* **1965**, *140*, A1133−A1138.
(3) Perdew, J. P.; Zunger, A. *Phys. Rev. B* **1981**, *23*, 5043−5079.
(4) Langreth, D. C.; Perdew, J. P. *Phys. Rev. B* **1980**, *21*, 5469−5493.
(5) Perdew, J. P.; Wang, Y. *Phys. Rev. B* **1986**, *33*, 8800−8802.
(6) Perdew, J. P.; Burke, K.; Ernzerhof, M. *Phys. Rev. Lett.* **1996**, *77*, 3865−3868.
(7) Becke, A. D. *J. Chem. Phys.* **1993**, *98*, 5648−5652.
(8) Lee, C.; Yang, W.; Parr, R. G. *Phys. Rev. B* **1988**, *37*, 785−789.
(9) Stephens, P. J.; Devlin, F. J.; Chabalowski, C. F.; Frisch, M. J. *J. Phys. Chem.* **1994**, *98*, 11623−11627.
(10) Helgaker, T.; Jorgensen, P.; Olsen, J. *Molecular Electronic-Structure Theory*; Wiley, 2000.
(11) Fuchs, M.; Niquet, Y. M.; Gonze, X.; Burke, K. *J. Chem. Phys.* **2005**, *122*, 094116.
(12) Grüning, M.; Gritsenko, O. V.; Baerends, E. J. *J. Chem. Phys.* **2003**, *118*, 7183−7192.

(13) Gori-Giorgi, P.; Seidl, M.; Vignale, G. *Phys. Rev. Lett.* **2009**, *103*, 166402.
(14) Seidl, M.; Gori-Giorgi, P.; Savin, A. *Phys. Rev. A* **2007**, *75*, 042511.
(15) Gori-Giorgi, P.; Seidl, M. *Phys. Chem. Chem. Phys.* **2010**, *12*, 14405−14419.
(16) Malet, F.; Gori-Giorgi, P. *Phys. Rev. Lett.* **2012**, *109*, 246402.
(17) Chen, H.; Friesecke, G. Preprint.
(18) Malet, F.; Mirtschink, A.; Giesbertz, K. J. H.; Wagner, L. O.; Gori-Giorgi, P. *Phys. Chem. Chem. Phys.* **2014**, *16*, 14551−14558.
(19) Monge, G. Histoire Acad. Sciences: Paris, 1781.
(20) Kantorovich, L. V. *Dokl. Akad. Nauk. USSR* **1940**, *28*, 212−215.
(21) Kantorovich, L. V. *Dokl. Akad. Nauk. USSR* **1942**, *37*, 199−201.
(22) Villani, C. *Optimal transport: Old and new*; Springer: Heidelberg, 2009.
(23) Cotar, C.; Friesecke, G.; Klüppelberg, C. *Comm. Pure Appl. Math.* **2013**, *66*, 548−599.
(24) Buttazzo, G.; Pascale, L. D.; Gori-Giorgi, P. *Phys. Rev. A* **2012**, *85*, 062502.
(25) Cotar, C.; Friesecke, G.; Pass, B. 2013, arXiv:1307.6540.
(26) Friesecke, G.; Mendl, C. B.; Pass, B.; Cotar, C.; Klüppelberg, C. *J. Chem. Phys.* **2013**, *139*, 164109.
(27) Mendl, C. B.; Lin, L. *Phys. Rev. B* **2013**, *87*, 125106.
(28) Vuckovic, S.; Wagner, L. O.; Mirtschink, A.; Gori-Giorgi, P. In preparation.
(29) Lieb, E. H. *Int. J. Quantum Chem.* **1983**, *24*, 243−277.
(30) Seidl, M. *Phys. Rev. A* **1999**, *60*, 4387−4395.
(31) Seidl, M.; Perdew, J. P.; Levy, M. *Phys. Rev. A* **1999**, *59*, 51−54.
(32) Gangbo, W.; McCann, R. J. *Acta Math.* **1996**, *177*, 113−161.
(33) Hoffmann-Ostenhof, M.; Hoffmann-Ostenhof, T.; Østergaard Sørensen, T. *Ann. Henri Poincaré* **2001**, *2*, 77−100.
(34) PHG. http://lsec.cc.ac.cn/phg, accessed August 1, 2013.
(35) MOSEK. http://www.mosek.com, accessed August 1, 2013.
(36) Kolos, W.; Roothaan, C. C. *Rev. Modern Phys.* **1960**, *32*, 219−232.
(37) Cohen, A. J.; Mori-Sánchez, P.; Yang, W. *Chem. Rev.* **2012**, *112*, 289−320.